IFSCC 2025 full paper (2025-1665)

Application and Effect Evaluation of EGCG Biomimetic Exosomes in Anti-wrinkle Cosmetics

Xinhui Zhou [1,2*], Zeting Huang [1,3], Weihua Peng [1], Weiqiu Wen [2], , Guanhai Wang [3*]

[1] China Guangzhou Zhongzhuang Meiye Cosmetics Co., Ltd. Guangzhou, China

[2] Huangpu Institute of Materials, Guangzhou, China

[3] School of Pharmacy, Guangdong Medical University, Dongguan, China

[*] To whom correspondences should be addressed: zhouxh_lee90@126.com

1. Introduction

Recent years have witnessed rapid development of nano-preparation technology represented by nano-carrier, which has risen to be the frontier and hot spot in the international medical community and demonstrated huge development and application potentials in the fields of transdermal drug delivery and functional cosmetics. Nanocarrier technology can promote transdermal penetration of functional actives with low solubility and poor stability and prevent damage to the skin barrier function, making it an ideal technology to facilitate transdermal drug delivery. Inspired by the structures and properties of natural organisms, the biomimetic nanodrug delivery system is changing the design approach of traditional drug delivery systems with the merits of enhancing biocompatibility and significantly increasing therapeutic efficacy[1]. Based on the biological properties of biomimetic units, biomimetic nanodrug delivery systems can be roughly divided into four categories: nanodrug delivery systems based on natural biological macromolecules[2-4], cell and cell membrane-related drug delivery systems[5-7], extracellular vesicle drug delivery systems such as exosomes[8-10], and nanodrug delivery systems that mimic biological structures[11-15].As a promising biomimetic drug delivery nanomaterial, biomimetic exosomes[11-12] has been applied in frontier treatment research in recent years.

Biomimetic exosomes are cellular exosome-like structures with high loading capacity and precise targeting property developed through artificial structure mimicry and functionalized molecular surface modification.We developed a biomimetic exosome that realizes high content loading and highly efficient targeted transmembrane delivery of the cosmetic efficacy ingredient epigallocatechin gallate (EGCG). EGCG, a major catechin found in green tea, known for its remarkable antioxidant, anti-inflammatory and anti-photoaging properties, possesses immense potential as an active ingredient in cosmetic products[16-18]. However, its inherent limitations have hindered its successful utilization in skincare formulations, such as poor stability[18] and limited skin penetration. To overcome these obstacles, the biomimetic exosomes has been explored as a promising delivery system for EGCG. The biomimetic exosome not only solves problems of EGCG like its instability, proneness to change property and deactivate, and difficulty to transdermal absorption, but also has stronger cell recognition ability.

2. Materials and Methods

2.1. Materials

HACAT cells were purchased from Cell Bank of Chinese Academy of Science (Shanghai). Chemical reagents including Lecithin, cholesterol and glycerol were sourced from Energy Chemical (Shanghai, China). EGCG were obtained from Sigma-Aldrich (Beijing, China). Tris(hydroxymethyl)aminomethane, Ethanol, Elastase(Enzyme activity 30 U/mg) and N-Succinyl-Ala-Ala-Ala-p-nitroanilide(AAAPVN) were purchased from Macklin (Shanghai, China). FBS, MTT, DAPI, and 2′,7′-dichlorofluorescein diacetate (DCFHDA) were procured from Carlsbad (USA). All the reagents utilized were of analytical grade and employed as received.

2.2. Preparations of Biomimetic Exosomes

EGCG biomimetic exosomes (BE-EGCG) was prepared by the bottom-up assembly method. Briefly, Lecithin (2g), cholesterol (0.15g) and EGCG (5g) were added to the ethanol (30mL) and dissolved completely as the lipid solution. In order to recostitute the mitochondrial targeting protein on the EGCG biomimetic exosomes membrane, the mitochondrial targeting protein (0.014g) was incorporated into PBS buffer (92.836g) as the protein solution. Keeping below 25°C, the lipid solution was added dropwise to the protein solution under agitation, and the homogenization was continued at high speed (9000 rpm) for 5min. After that, the prepared BE-EGCG was self-assembled through removing ethanol using a rotary evaporator. By comparison, EGCG-loaded liposome (L-EGCG) and free EGCG solution were futher prepared on the premise that the content of EGCG in the samples was consistent. Typically, the preparation of L-EGCG was similar to that of BE-EGCG mentioned above, except that PBS buffer was used instead of the protein solution. And the free EGCG solution was prepared by dissolving EGCG (5g) into PBS buffer (95g). The particle size and morphology of BE-EGCG were observed by tranmission electron microscopy (TEM) (HT7700, Hitachi, Japan).

2.3. Encapsulation capacity

200 μL of EGCG biomimetic exosomes(BE-EGCG) was transferred to the ultrafiltration (MWCO 3500Da), and the free EGCG of biomimetic exosomes was collected by filtration centrifugation (9000 rpm, 30min) and determined by high performance liquid chromatography (HPLC) (LC-20A, Shimadzu, Japan). Another sample was taken and methanol was added, and the emulsion was broken by ultrasonicaition for 30 min, and the content of EGCG was determined by HPLC. The HPLC system was used a C18 column, and the mobile phases were methanol and water with 2% acetic acid, and the detectin wavelength was 272 nm. The encapsulation effciency (*EE*) for the active ingredient in the BE-EGCG was as follows:

$$EE(\%) = (1 - \frac{C_0}{C_1}) \times 100\%$$

where C_1 represents the total weight of the EGCG in the prepared BE-EGCG, C_0 represents the weight of the free EGCG.

2.4. Construction of cell models for oxidative damage (UV irradiation)

HACAT cells were grown in standard RPMI medium, supplemented with 10% fetal calf serum, 2 mM L-glutamine and antibiotics at 37 °C in 5% CO_2. To study the protection of EGCG, HACAT cells were exposed to UVA (10 J/m2, 390 nm) for 30 min.

2.5. Intracellular ROS scavenging ability

ROS level was evaluated by CLSM in HACAT cells. HACAT cells were cultured in a 35 mm confocal dish (1×10^5 cells/well) 24 h and exposed to UVA irradiation for 30 min. The cells after UVA irradiation were grouped and dosed. The experiment was set up with 4 groups : group 1(EGCG 0 μg/mL, UV irradiation),group 2(EGCG 10 μg/mL, UV irradiation) and group 3(L-EGCG 10 μg/mL, UV irradiation), and group 4(BE-EGCG 10 μg/mL, UV irradiation). 1 mL of sample was added to each well, separately. After the administration was completed, the well plates were placed in a 37 °C incubator and incubated in the dark for 24 hours.The cells were then fixed using 4% paraformaldehyde for 10 min and rinsed with PBS. Afterward, they were treated with DCFH-DA (10 μM) for 30 min and examined using a CLSM (Ex: 488 nm, Em: 500 nm-540 nm).

2.6. Inhibition rate of elastase activity

Four sets of clean test tubes were taken, labeled as A, B, C and D. 25μL test sample was added to test tubes A and B, 25μL deionized water was added to test tubes C and D. Then 0.171U/mL porcine pancreatic elastic proteinase solution 25μL was added to test tubes A and C, respectively. Add 25μL of Tris-HCl buffer solution with pH=8.0 in test tubes B and D respectively. 2mM AAAPVN solution 50μL was added to the four test tubes, mixed and placed at room temperature for 15min, and then the absorbance was measured at 420nm with an enzyme label.

$$\text{Elastase inhibition rate (\%)} = (1-\frac{OD_C - OD_D}{OD_A - OD_B})\times 100\%$$

In the formula OD_A is the OD value of the sample solution, OD_B is the OD value of the sample blank, OD_C is OD value of the control sample solution, OD_D is the OD value of the blank control sample.

2.7. Determination of cell endocytosis

EGCG itself did not have fluorescent properties, so in this experiment, EGCG-FITC was first synthesized, and then EGCG-FITC liposomes and EGCG-FITC biomimetic exosomes were prepared. The prepared fluorescent labeled samples were stored at 4℃ away from light. EGCG-FITC was green fluorescence, and FITC channel was selected in the experiment. HACAT cells were cultured in a 10 mm confocal dish (5×10^4 cells/well) at 5%CO_2 and 37℃ for 24h. The cells were cleaned with PBS, and added 10 μL of 100 μg/mL samples in each well, respectively. Finally, to stain the nuclei, DAPI was added and the samples were incubated for an additional 30 min. The endocytosis of the treated cells was observed at excitation wave 488nm and emission wave 520nm at 30min, 1h, 2h and 4h, respectively.

2.8. Determination of Skin Penetration

EGCG biomimetic exosomes, EGCG, collagen and hexapeptide-9 aqueous solution were applied to artificial skin-on-a-chip models[19-20], with three parallel experiments set up for each group. 400 μL of the test solution was added to the upper surface of each model, and 800 μL of culture medium solution was added to the lower chamber. Subsequently, the skin models were placed in a culture box and incubated in the dark for 24 hours. The test substances and culture medium in the models were then discarded, and the model surfaces were washed twice with DPBS to remove any excess substances. The models were then fixed in 4% paraformaldehyde for 24 hours, dehydrated in 10%, 20%, and 30% sucrose solutions respectively, until the models sank to the bottom in the 30% sucrose solution, indicating the completion of dehydration. The models were embedded in OCT and frozen sections were made with a thickness of 10 μm. The fluorescence in the sections was observed to evaluate the retention effect of the four substances in the skin-on-a-chip models.

2.9. Human efficacy evaluation

The EGCG biomimetic exosomes prepared in 2.2 were added to the test cream at a mass percentage of 0.5% . 35 healthy volunteers aged 30 to 50 years old, who had problems such as dry, rough, loose facial skin and fine lines or wrinkles around the eyes, were selected for the human trial to evaluate the anti-aging efficacy. The specific screening method was as follows: the baseline value of the skin moisture content of the test area of the volunteers measured by the capacitance method skin moisture meter was ≤ 60 (Corneometer Unit, C.U.), the skin glossiness Gloss DSC was ≤ 7 a.u., the facial skin was loose and inelastic with F4 > 6 and R2 ≤ 65%. According to the "Atlas of Skin Aging (Asian People)", the crow's feet, under-eye fine lines, nasolabial folds and forehead wrinkles were ≥ grade 2, and the pores were ≥ grade 2. The instrument test and self-assessment methods were employed to test parameters such as the moisture content of the stratum corneum, glossiness, translucency, smoothness/roughness, firmness F4, elasticity R2, dermal density/thickness, wrinkle parameters (crow's feet, under-eye fine lines, nasolabial folds and forehead wrinkles), jawline angle, eyelid droop angle and pore area ratio of the skin of 35 volunteers before using the product and 4 weeks after using the product, in order to verify the effects of the product.

3. Results

3.1. Preparation and characterization of Biomimetic Exosomes

The morphology of the EGCG biomimetic exosomes was observed by TEM. As shown in **Figure 1**, the biomimetic exosomes-like nanoparticles exhibited a spherical shape with diameters ranging from 70-80 nm. The biomimetic exosomes' approaches for bottom-up assembly include modifying liposomes with membrane proteins, embedding specific proteins into NPs, reassembling cellular lipid fractions, or creating fully synthetic exosome particles[12]. The *EE* of EGCG in the biomimetic exosomes was measured by HPLC and reached to 80%.

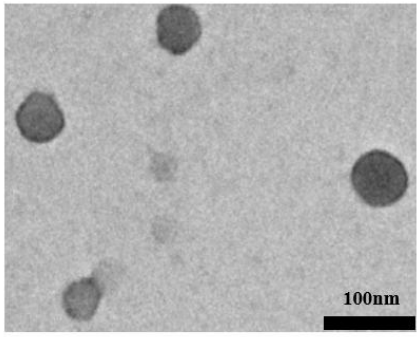

Figure 1. TEM images of EGCG biomimetic exosomes-like nanoparticles.

3.2. Antioxidant Capacity

Antioxidant activity is a crucial parameter for assessing the efficacy of cosmetics. Reactive oxygen species participate in the signaling pathway of skin matrix formation and degradation. Oxidative stress affects skin aging by reducing proteasome activity, damaging DNA and its repair system, and damaging telomeres. In this work, intracellular ROS scavenging activities were evaluated the antioxidant activity of EGCG biomimetic exosomes(BE-EGCG), EGCG liposomes (L-EGCG) and free EGCG as the control groups.

As shown in **Figure 2**, strong green fluorescence was observed in UV irradiated control group, indicating high intracellular ROS level. In contrast, the green fluorescence intensity of BE-EGCG group was obviously weaker than that of control group. Owning to donating

electrons or hydrogen atoms in molecules, EGCG showed good antioxidant capacity and quench these highly reactive free radicals. Moreover, EGCG can bind and chelate metal ions, such as iron and copper, that are involved in ROS generation through Fenton and Haber-Weiss reactions. Moreover, exosome-like substances had better transmembrane effects and biological activities, could enhanced the activity of intracellular antioxidant enzymes, and eliminated intracellular reactive oxygen species. Combined these protective effects, BE-EGCG had superior antioxidant activity.

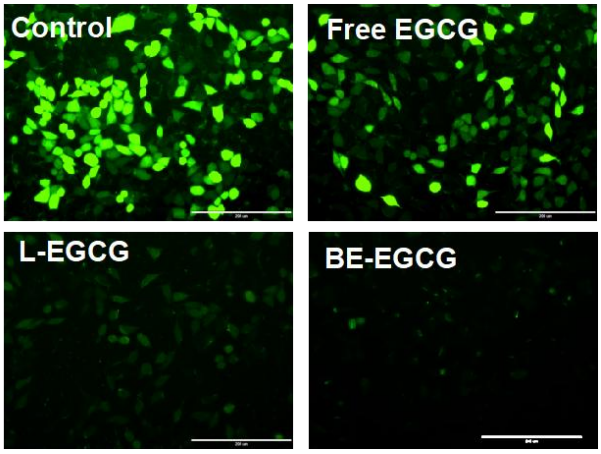

Figure 2. CLSM images of HACAT cells of EGCG , EGCG liposomes and biomimetic exosomes. DCFH-DA probe was used to stain intracellular ROS. Scale bar: 100 μm.

3.3. Inhibition rate of elastase activity

Inhibition rates of elastase by the different concentrations of EGCG , L-EGCG and BE-EGCG were shown in Figure 3. Under the conditions of this experiment, different preparations of EGCG at the detection concentration of 0.1% - 1.0% all had a significant inhibitory effect on the activity of elastase. Compared with the elastase inhibition rate under the same concentration, when the BE-EGCG preparation was prepared by the 2.2 at 0.5% test concentration, the elastase inhibition rate of BE-EGCG was enhanced by 16.2% over the L-EGCG, and 28.0% over free EGCG.

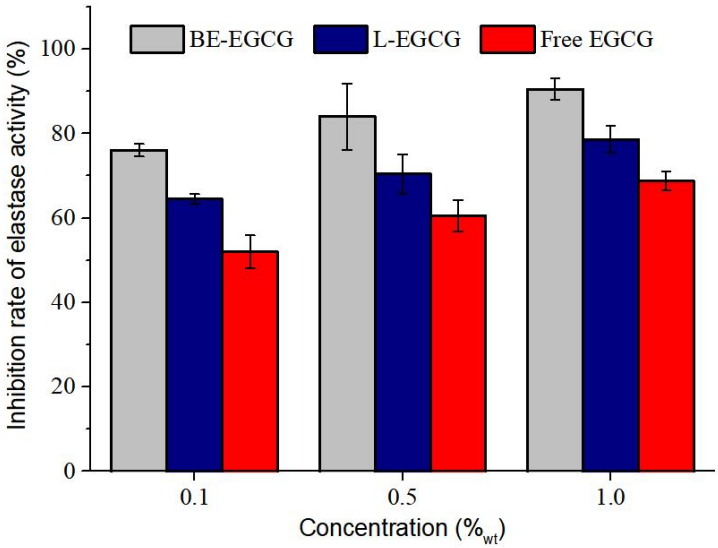

Figure 3. Inhibition rate of elastase by the different concentrations of EGCG , L-EGCG and BE-EGCG. All these prearations contain 5% EGCG.

3.4 Cell Endocytosis Test

Fluorescence imaging of drug entosis was performed by confocal laser microscopy under specific excitation waves of FITC-EGCG. Figure 4 showed the immunofluorescence staining results of human immortalized epidermal cells. With the increase of administration time, the more FITC drugs exocytosis, the higher the intracellular fluorescence intensity. After 4 h, the target recognition and endocytotic rate of EGCG biomimetic exosomes on HACAT cells were enhanced by 63% over plain liposome coated by EGCG and 109.41% over free EGCG. These results indicated that EGCG biomimetic exosomes had higher cell recognition ability, and were more conducive to cell targeted absorption.

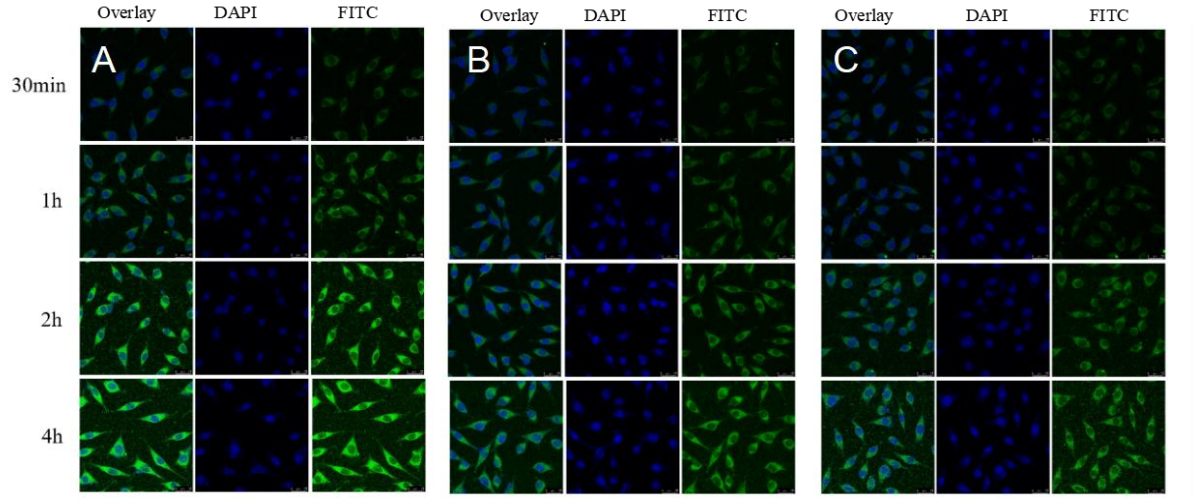

Figure 4. Immunofluorescence staining results of human immortalized epidermal cells (green fluorescence for target drug expression, blue fluorescence for nuclear staining). Group A was EGCG biomimetic exosomes, group B was EGCG ordinary liposomes. Group C was EGCG aqueous solution.

3.5. Skin Penetration Test

The skin permeation of four active substances (EGCG biomimetic exosomes, EGCG, collagen, and hexapeptide) in the skin-on-a-chip models was detected by fluorescence tracing technology for 24 hours. The results indicated that all the tested substances possessed transdermal permeation ability (Figure 5), but their distribution characteristics in each layer of the skin exhibited significant differences (Figure 6). EGCG biomimetic exosomes demonstrated unique transmembrane delivery advantages, with the fluorescence signal intensity in the epidermis being significantly higher than that of the other three groups. Specifically, it was 2.93 times higher than the EGCG group, 3.47 times higher than the collagen group, and 1.95 times higher than the hexapeptide-9 group, suggesting that this carrier system could significantly enhance the specific uptake of active components by epidermal keratinocytes. In the dermis, the permeation amount of EGCG exosomes was 2.45 times that of EGCG. Simultaneously, EGCG biomimetic exosomes also displayed excellent interlayer migration ability, with the relative fluorescence intensity in the dermis being significantly higher than that of the EGCG experimental group, and the accumulation curve in the epidermis-dermis junction area presented a gradient sustained-release characteristic. From the perspective of permeation kinetics, although collagen and hexapeptide-9 showed higher retention in the middle layer of the dermis, their bioavailability in the epidermis was significantly lower than that of EGCG biomimetic exosomes.In conclusion, EGCG biomimetic

exosomes had demonstrated remarkable superiority in promoting specific uptake in the epidermis, interlayer migration, and sustained-release ability in the dermis.

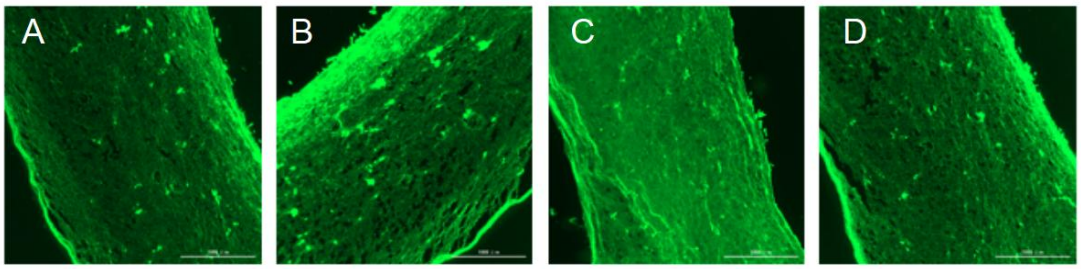

Figure 5. After 24 h, the retention of free EGCG (A), EGCG biomimetic exosomes(B),free collagen (C) and free hexapeptide-9 (D) in the skin-on-a-chip models.

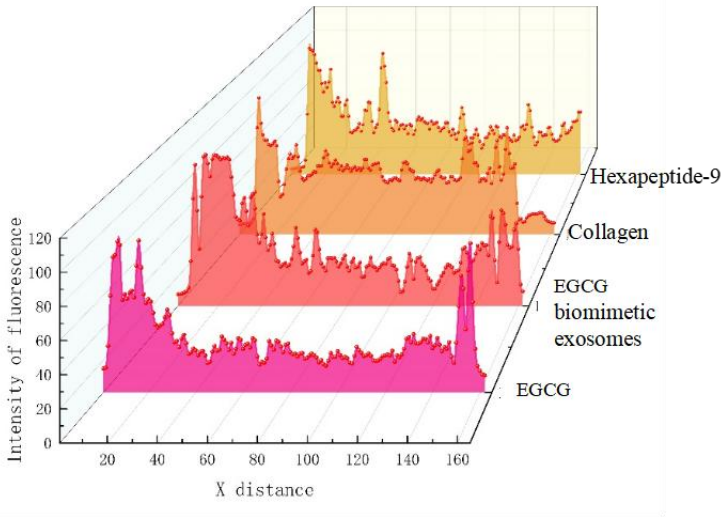

Figure 6. After 24 h, the distribution of four active substances in the skin-on-a-chip models.

3.6. Human efficacy evaluation

After 35 subjects used the face cream containing 0.5% EGCG biomimetic exosome for 4 weeks, Figure 4 showed this human 28-days trial effect. Compared with before usage, after 4 weeks of using the face cream,the significant changes were found within the test area: the R2 value and the F4 value was significantly improved by 16.63% and 17.58% ($p < 0.001$, $p < 0.001$), respectively; dermal densities were significantly increased by 52.34% ($p < 0.001$) and dermal thickness was significantly improved by 18.06% ($p < 0.001$); the value of the angle of opening of the outer corners of the eyes was significantly improved by 10.86% ($p < 0.001$); the angle of the mandibular line was significantly decreased by 4.22% ($p < 0.001$); the area of lateral canthal lines and its proportion were significantly reduced by 16.30% and 14.94% ($p < 0.001$, $p < 0.001$), respectively ; the area of fine lines under the eyes and its proportion were significantly reduced by 11.99% and 12.46% ($p < 0.001$, $p < 0.001$), respectively; the area of forehead wrinkles and its proportions were significantly reduced by 29.56% and 29.59% ($p = 0.001$, $p < 0.001$), respectively; and the linear light intensity of nasolabial folds was significantly reduced by 17.34% ($p < 0.001$).

Image Segmentation	W0	W4
Density of genuine leather	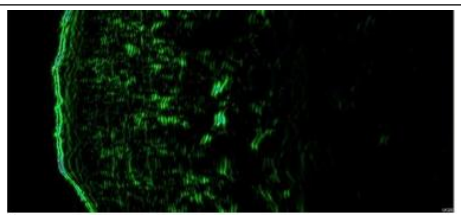	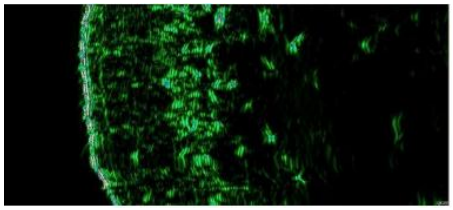
Subocular striae		
Crow's feet		
Maxillary line		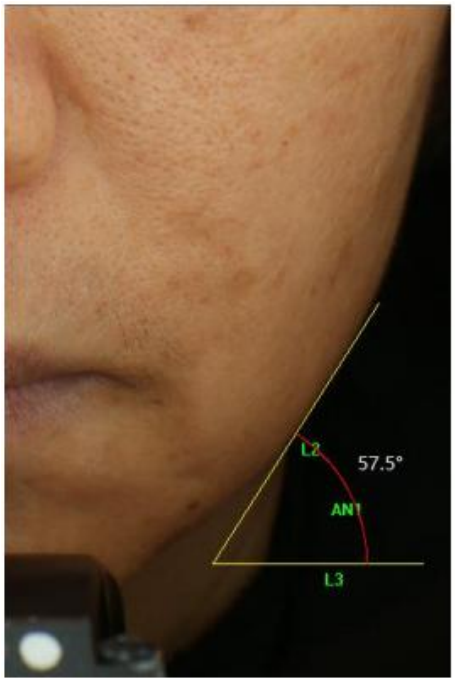
Forehead lines		

Figure 7. Imaging analysis performed in VISIA.

4. Discussion

Biomimetic nanoparticles are obtained by modification of natural materials or by chemical methods imitating the key characteristics of biological structures. They are similar to biologically related structures in chemistry, physics or morphology. Therefore, they exhibit excellent intelligent delivery performance in inert rejection, barrier overcoming and active effects, and can be used for more efficient and safe drug delivery. Biomimetic exosomes are cellular exosome-like structures with high loading capacity and precise targeting property developed through artificial structure mimicry and functionalized molecular surface modification. In the future, we will continue to load more active ingredients into the biomimetic exosomes, and conduct research on the application of it in the field of regenerative medicine.

5. Conclusion

In conclusion, this study demonstrates the potential of EGCG-biomimetic exosomes nanoparticles as an effective strategy to enhance the skin penetration of EGCG in cosmetic products. The developed EGCG-biomimetic exosomes nanoparticles effectively augment its pharmacological benefits related to ROS scavenging, cell endocytosis, inhibit elastase activity and promote collagen production. Moreover, the encapsulation of EGCG into biomimetic exosomes nanoparticles offers improved stability, greater skin permeation, and protection against oxidation. What's more, the face cream containing 0.5% EGCG biomimetic exosome has a significant anti-aging effect.

References:

[1] Mano J F, Choi I S, Khademhosseini A. Biomimetic interfaces in biomedical devices[J]. Advances Healthcare Materials, 2017, 6(15):1700761.

[2] Shah S, Dhawan V,Holm R, et al. Liposomes: advancements and innovation in the manufacturing process[J]. Advanced Drug Delivery, 2020, 154-155:102-122.

[3] Bottcher S E, Lou J C, Best M D, Liposome triggered content release through molecular recognition of inositol trisphosphate. Chemical Communication, 2022, 58(28):4520-4523.

[4] Katyal P, Meleties M, Montelare J K. Self-assembled protein- and peptide-based nanomaterials[J]. ACS Biomaterials Science & Engineering, 2019, 5(9):4132-4147.

[5] Mohale S, Kunde S S, Wairkar S. Biomimetic Fabrication of nanotherapeutics by leukocyle membrance cloaking for bone therapy[J]. Colloids and Surfaces B: Biointerfaces, 2022, 219: 112803.

[6] Chen Y T, Zhu M R, Huang B T, et al. Advances in cell membrane-coated nanoparticles and their applications for bone therapy[J]. Biomaterials Advances, 2023, 144: 213232.

[7] Oroojalian F, Beygi M, Baradaran B, et al. Cell membrane biominetic nanoparticlcs for inflammation and cancer targeting cancer therapy[J]. Small, 2021, 17(12): 2006484.

[8] GARAEVAL L, KAMYSHINSKY R, KIL Y, et al. Delivery of functional exogenous proteins by plant derived vesicles to human cells in vitro[J]. Scientific Reports, 2021, 11: 6489.

[9] HE B Y, HAMBY R, JIN H L. Plant extracellular vesicles: Trojan horses of cross-kingdom warfare [J]. FASEB Bioadvances, 2021, 3(9): 657-664.

[10] XU X H, YUAN T J, DAD A H, et al. Plant exosomes as novel nanoplatforms for microRNA transfer stimulate neural differentiation of stem cells in vitro and in vivo [J]. Nano Letters, 2021, 21(19): 8151-8159.

[11] Kumar S, Karmacharya M, Michael I J, et al. Programmed exsome fusion for energy

generation in living cells[J]. Nature Catalysis, 2021, 4(9): 763-774.

[12] Xu Xiao, Xu Limei, Wen Caining, et al. Programming assembly of biomimetic exosomes: An emerging theranostic nanomedicine platform[J]. Materials Today Bio, 2023, 22: 100760.

[13] Zhang J W, Li D D, Zhang R, et al. Delivery of microRNA-21-sponge and pre-microRNA-122 by MS2 virus-like particles to therapeutically target hepatocellular carcinoma cells[J]. Experimental Biology and Medicine, 2021, 246(23):2463-2472.

[14] Olszewska-Widdrat A, Benet M, Mickoleit F, et al. Bactcriophage-templated assembly of magnetic nanoparticlcs and their actuation potential[J]. ChemNanoMat, 2021, 7(8):942-949.

[15] Yang G Z, Liu Y, Jin S, et al. Development of core-shell nanoparticlcs drug delivery systems based on biomimetic mineralization[J]. ChemBioChem, 2020, 21(20):2871-2879.

[16] J. Xu, H. Zhang, M. Deng, H. Guo, L. Cui, Z. Liu, J. Xu, Food Research International, 2024, 186: 114365.

[17] X. Wang, L. Han, S. Qu, L. Feng, S. Liang, C. Wei, X. Liu, X. Dang, International Journal of Biological Macromolecules, 2024, 268: 131682.

[18] T. Liu, M. Liu, H. Liu, Y. Ren, Y. Zhao, H. Yan, Q. Wang, N. Zhang, Z. Ding, Z. Wang, Food & Function, 2021,12: 7126-7144.

[19] Vijayan S M , Baierl M , Gen T ,et al.Intradermal and transdermal absorption of beta-naphthylamine and N-Phenyl-beta-naphthylamine in a viable human skin model[J].Toxicology in Vitro, 2024, 101(000).

[20] Hashimoto N , Nakamichi N , Yamazaki E ,et al.P-Glycoprotein in skin contributes to transdermal absorption of topical corticosteroids[J].Int J Pharm, 2017, 521(1-2):365-373.